

Effective Plans for Hospital System Response to Earthquake Emergencies

Luis Ceferino¹, Judith Mitrani-Reiser^{2,3}, Anne Kiremidjian¹, Gregory Deierlein¹, and Celso Bambarén⁴

¹Department of Civil and Environmental Engineering, Stanford University

²National Institute for Standards and Technology

³Department of Civil Engineering, Johns Hopkins University

⁴Universidad Peruana Cayetano Heredia

September 18, 2019

Abstract

Hospital systems play a critical role in treating injuries and preventing additional deaths during disaster emergency response. Natural disasters hinder the ability of hospital systems to operate at full capacity. Therefore, it is important for cities to develop policies and standards that enable hospitals' continuous operations to provide patients with timely treatment and ensure urban resilience. Here, we present a methodology to evaluate emergency response based on a probabilistic model that assesses the loss of hospital functions and quantifies multiseverity injuries as a result of earthquake damage. The proposed methodology is able to design effective plans for patient transferal and allocation of medical resources using an optimization formulation. This methodology is applied to Lima, Peru, subjected to a disaster scenario based on the M 8.0 earthquake that occurred there in 1940. Our results show that the spatial distribution of health service demands mismatches the post-earthquake capacities of hospitals, leaving large zones on the periphery of Lima significantly underserved. This study demonstrates how emergency plans that leverage hospital-system coordination can address this demand-capacity mismatch, enabling effective patient transfers, ambulance usage, and deployment of emergency medical teams.

Hospital systems are at the core of disaster resilience because they must provide timely critical healthcare services to communities during and after an emergency response.¹ Because cities are becoming larger and more densely populated, natural disasters are impacting public health on a larger scale. A database including the most 21,000 devastating disasters worldwide since 1900 indicates that 50% of disasters with the largest number of injuries occurred only during the last 20 years.² Natural disasters such as earthquakes, landslides, floods, typhoons put heavy demands on hospital systems because these disasters can cause thousands or even tens of thousands of injuries in a short timespan (Figure 1). At the same time, natural disasters cause massive disruptions to hospital systems by damaging their supporting infrastructure. For example, the M 7.6 1999 Turkey

Corresponding author: Luis Ceferino. E-mail: lceferinor@gmail.com
Preprint submitted to Nature Communications

35 earthquake caused around 50,000 injuries in Izmit and disrupted 10 major hospitals, which required
36 relocation of most patients from these hospitals.³

37 Because hospital systems are so critical, the World Health Organization (WHO) and Pan-
38 American Health Organization (PAHO) urge countries to institute policies to strengthen hospi-
39 tal capacities and enhance coordination in the hospital system to make efficient use of resources
40 at national and regional levels during emergency response.^{4,5} To effectively develop measures
41 for capacity-enhancing prioritization and resource sharing and allocation, national and regional
42 governments require information based on robust methodologies that can characterize hospitals’
43 emergency response as an interconnected system on a large urban scale.

44 However, most previous studies have primarily focused on modeling emergency response only at
45 single-hospital scale as opposed to characterizing the response of hospital systems on a large urban
46 scale. Some of these studies relied on disaster analytics to evaluate post-disaster functionality of the
47 supporting infrastructure in the individual hospitals.⁶⁻⁹ Other studies used emergency medicine
48 modeling tools, such as discrete event simulation (DES) and flow models, to characterize emergency
49 response and evaluate post-disaster resource allocation but also at a single-hospital scale.¹⁰⁻¹³ Lack
50 of methods and high-resolution disaster risk data have hindered the extension of single-hospital
51 scale analyses to system-level analyses on an urban scale. As a result, regional emergency response
52 policies have not effectively addressed capacity-enhancing prioritization and resource sharing and
53 allocation in hospital systems, especially in large and complex urban centers.

54 Here, we present findings from a methodology that characterizes the disaster emergency response
55 of hospital systems on a large urban scale. Our integrative methodology combines models of
56 multiseverity earthquake casualty estimation^{14,15} and post-earthquake hospital functionality with a
57 proposed network flow model for hospital systems. We focus on seismic hazard because earthquakes
58 are the natural disasters that have caused the largest number of injuries in most countries (Figure 1).
59 The methodology is applied to Lima, Peru, based on a M 8.0 earthquake and includes an evaluation
60 of effective emergency plans for allocation of hospital resources and patient transfers. We selected
61 Lima because it has a high seismic risk and it has recently built a unique dataset containing high-
62 resolution hospital vulnerability. We use citywide data on the seismic vulnerability of more than
63 1.5 M buildings in Lima to estimate casualties and data including the seismic vulnerability of 41
64 public hospital campuses (composed of +700 buildings) and their respective operating rooms and
65 ambulance resources.^{9,16,17}

66 We propose a metric based on patient waiting times and effective use of ambulance patient
67 transfers as a performance measure for developing emergency response plans. Our focus is on
68 high-severity injuries that require surgical procedures. We evaluate the spatial distributions of
69 high-severity injuries in the city at a higher spatial resolution (i.e., 1kmx1km) than other widely
70 used methods.¹⁸ Then, we compare the spatial distribution of casualties with the distribution of
71 functional operating rooms in the hospital system, identifying the zones more likely to be under-
72 served during the emergency response. Combining the network flow model with an optimization
73 formulation, we assess the performance of four alternative emergency response plans to treat the
74 patients in the city.

75 The first and second emergency plans are baseline strategies with limited levels of coordination.
76 In both strategies, hospitals without available operating resources will use their own ambulances to
77 transfer patients, but in the first strategy, patients will only be sent to the closest working hospital,
78 whereas in the second strategy, patients will be sent to the hospital with the largest number of
79 functional operating rooms.

80 The third and fourth emergency plans are strategies with higher levels of coordination that use
 81 the optimization formulation on the system performance metric. In both strategies, all hospitals
 82 will share ambulance resources across the system to transfer patients according to post-earthquake
 83 needs, but in the third strategy, the system only uses the residual operating room capacities in
 84 the hospitals, whereas in the fourth strategy, emergency medical teams (EMTs) supply the system
 85 with additional mobile operating rooms in key locations in the city. Through the Action Plan for
 86 Humanitarian Assistance, the WHO and PAHO require countries to elaborate policies for deploying
 87 ETMs to assist people affected by emergencies and disasters,^{19,20} thus, this study aims to directly
 88 inform policies for EMT deployment in countries with high seismic risk.

89 We analyze the behavior and performance of these four plans during the emergency response and
 90 discuss their implications in terms of patient treatment times, ambulance usage, and patient trans-
 91 fers. We utilize traffic data to show the most important roads for patient transfers from localized
 92 zones with lower hospital capacity to zones with higher capacity in the city. This research repre-
 93 sents a first-cut assessment on the effectiveness of emergency response policies to inform city-scale
 94 decision-making that leads to more effective treatment of patients during an emergency response
 95 to a major earthquake.

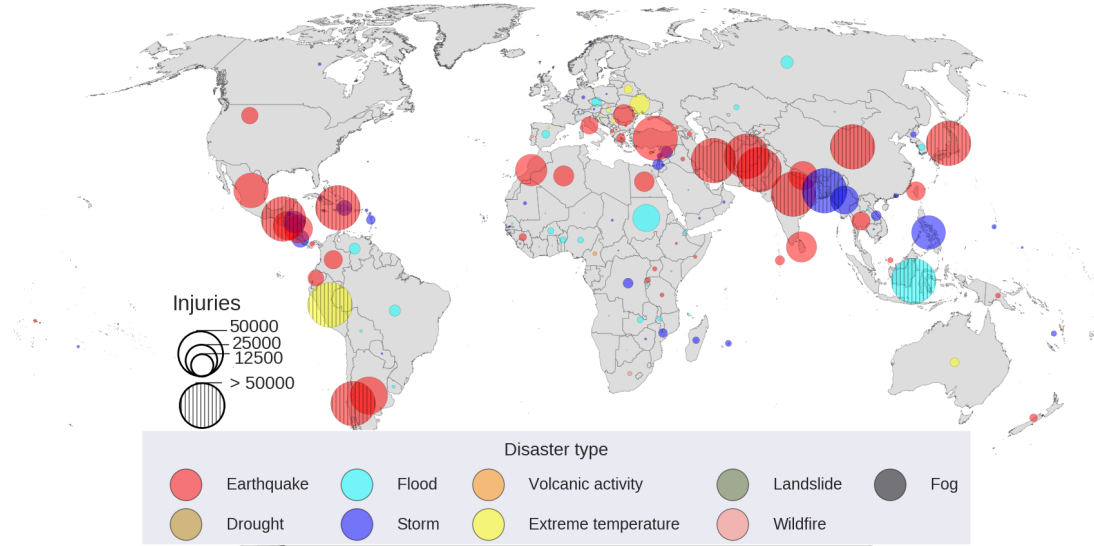


Figure 1: Per-country distribution of disasters with the highest number of injuries since 1900. The sizes of the circles indicate the relative number of injuries and the colors indicate the natural disaster type. Since 1900, 117 countries that experienced at least one natural disaster with more than 100 injuries. Earthquakes were the natural disaster with largest injury tolls in 45 of these countries, followed by storms in 38 of these countries. Earthquake events can cause large number of injuries suddenly. For example, the 2008 Great Sichuan earthquake injured more than 368k people in only two minutes. Data from EM-DAT.²

96 **1 Results**

97 We applied our methodology to Lima, a large city with a population close to 10 million people,²¹
 98 where previous large earthquakes have caused large numbers of casualties.^{22,23} Because the last

99 large earthquake in the region occurred more than 40 years ago, studies indicate that the city is
 100 currently exposed to high hazard of large-magnitude earthquakes.^{24,25} Using our proposed method-
 101 ology, we characterize the emergency response and evaluate response plans to effectively to treat
 102 patients in Lima after an earthquake scenario of large magnitude occurring in the near future. This
 103 earthquake scenario was simulated according to the seismotectonics of the 1940 M 8.0 earthquake,
 104 which occurred in close proximity to Lima.²⁶ Figure 2 shows the estimated rupture area of the 1940
 105 earthquake and its proximity to the city. Our methodology estimates the impact of this disaster
 106 scenario on the demands on healthcare by quantifying earthquake casualties and on the capacity
 107 of healthcare by quantifying the post-earthquake reduction in functionality in the hospital system.
 108 The results of applying our methodology are discussed here and the details of the methodology
 109 formulation, workflow and required data are described in the Methods section.

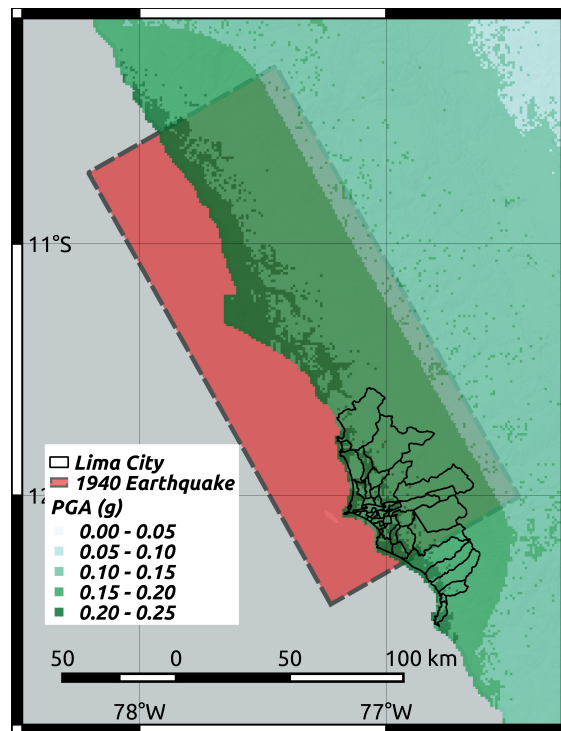


Figure 2: Earthquake scenario representing the M 8.0 1940 earthquake in Lima. The earthquake occurred in the subduction fault in the coast of Lima and caused widespread damage to the city.^{22,27} The estimated area of fault rupture is shown in red. The edge dimensions were estimated with empirical formulas.²⁸ The fault plane dips 15°, where the edge underneath the coast is deeper than the edge under the ocean. The median peak ground acceleration (PGA) is also estimated with empirical formulas.²⁹ The shaking attenuates for regions further away from the rupture in the fault plane. Lima city and its districts are delimited by the black shapes.

110 1.1 Earthquake Casualties

111 We found that on average close to 4.7k people will require surgical procedures in operating rooms
 112 after the M 8.0 earthquake. This estimate results from applying a probabilistic model that utilizes
 113 high-resolution building seismic vulnerability data, population distribution and soil conditions to

114 evaluate multiseverity earthquake casualties caused by widespread building damage^{14,15} (see Meth-
 115 ods). Earthquake injuries can have different severity degrees, ranging from small bruises to more
 116 serious spinal cord injuries.³⁰⁻³⁴ The 4.7k patients requiring surgical procedures will have high
 117 severity injuries such as compound bone fractures, punctured organs or crush syndrome with open
 118 wounds, thus they require timely interventions for stabilization and treatment.

119 Our results are designed for a nighttime scenario, when most people are inside residential build-
 120 ings, because residential infrastructure is particularly vulnerable in Lima. Predominantly the city's
 121 periphery has vulnerable residential infrastructure as a result of poor construction practices and
 122 lack of seismic code enforcement.^{35,36} Figure 3a shows the spatial distribution of the average num-
 123 ber of patients that will require the surgical procedures. A comparison with the spatial distribution
 124 of nighttime population density in Lima (Figure 9) indicates that most of these patients are located
 125 in high-density zones. However, the ratio between the number of injured people and the total num-
 126 ber of people follows a different pattern (Figure 3b). The spatial distribution of this ratio reflects
 127 the uneven distribution of ground shaking intensities and seismic vulnerabilities of buildings in the
 128 city. It shows that people living closer to the coastline and in the city's peripheral zones have
 129 higher earthquake injury risk as a result of higher ground shaking (Figure 2) and more vulnerable
 130 buildings, respectively.

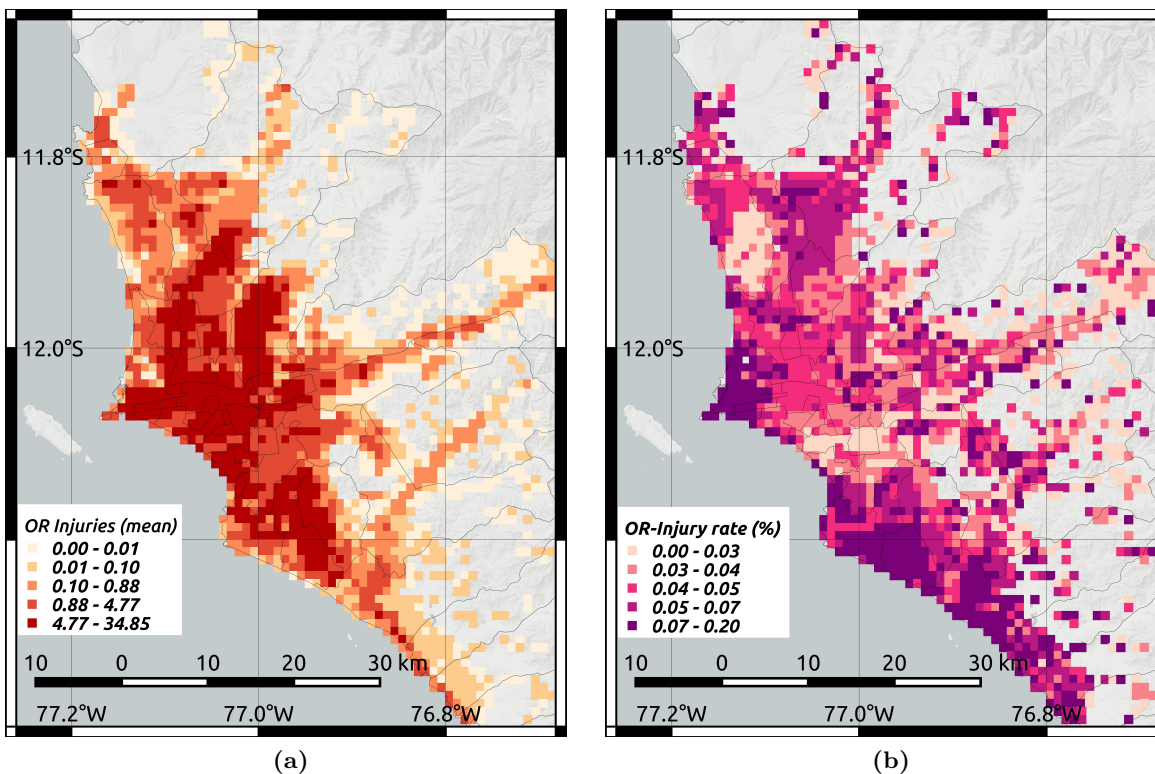


Figure 3: Casualty scenario for M 8.0 earthquake occurring at nighttime in Lima. (a) Spatial distribution in km² of earthquake injuries requiring surgical procedures after the M 8.0 seismic event. (b) Spatial distribution of earthquake injury ratios, i.e., number of injuries as a percentage of the population per km². The intervals in the two plots represent quintiles (5-quantile) on the spatial data.

1.2 Post-earthquake Hospital Capacity

We found that on average only 93 of 182 total hospital operating rooms (51%) will be functional after the M 8.0 earthquake. This estimate results from performing a probabilistic earthquake simulation on a high-resolution dataset (see Methods). The dataset includes the structural vulnerabilities of +700 buildings belonging to 41 healthcare campuses,¹⁶ the operating room resources, and “Hospital Safety Index” (HSI) of each campus. HSI is a metric created by WHO to measure post-disaster functionality potential due to multiple factors such as backup water, power, medical resources and hospital accessibility.³⁷ This unique dataset in combination with the earthquake simulation enables us to capture the residual hospital functionality on a large urban scale.

Figure 5a shows the spatial distribution of both the operating rooms in the dataset and the average predictions of operating rooms after the earthquake. Both spatial distributions are heavily uneven across the city. In the dataset, 95 operating rooms (52%) are concentrated in only four centric districts, Lima, Breña, La Victoria and Jesús María, whose summed areas represent less than 2% than the total area of the city. The earthquake slightly worsens such a resource centralization due to the non-uniform spatial distribution of earthquake shaking and the variations in the vulnerabilities of hospitals’ buildings according to their construction age and standards or structural types (Figure 11). As a result, we estimate that these four districts will have 55 functional operating rooms, 59% of the total functional operating rooms, in the emergency response.

Additionally, addressing the centralization issue can become even more critical because the number of injuries needing surgical procedures and the functional operating rooms are negatively correlated. Our findings show a strong correlation (-0.49) between the simulations of earthquake injuries and functional operating rooms across the system in the city (Figure 4). Such a large correlation indicates that an earthquake that injures a larger amount of people will likely be very destructive; thus, that scenario will also cause a heavier disruption to the hospital system.

1.3 Demand-capacity Mismatch of Health Services

We analyzed patient arrivals to the hospitals and found that patient distribution significantly mismatches the distribution of residual hospital resources after the earthquake. We assumed that search and rescue (SAR) teams, relatives, friends and neighbors will initially transport patients to the triage areas in the closest hospitals as it occurred after previous earthquakes.³⁸ Figure 5b shows the distribution of the total arrivals of the patients who will need surgical procedures in each hospital. In contrast to the distribution of functional operating rooms, injuries are mainly located in the periphery. Only 596 patients would arrive at the hospitals in the four centric districts highlighted in Figure 5b. Those patients represent only 13% of the total demand for surgical procedures. However, as described earlier, these four districts will concentrate 59% of the functional operating rooms available.

Such a mismatch in the distribution of demands and capacities creates localized health service imbalances leading to long patient waiting times, with particularly severe effects in the periphery. Emergency plans can play a key role in addressing this mismatch and improve the treatment effectiveness in the city if they either mobilize patients from lower-capacity zones to higher-capacity zones or supply lower-capacity zones with additional resources. We tested four emergency plans. Two of them are baseline strategies that only require limited coordination in the system, whereas the other two are strategies that require higher coordination at the system level. To evaluate their performance during the emergency response, we used a system metric based on city-wide patient

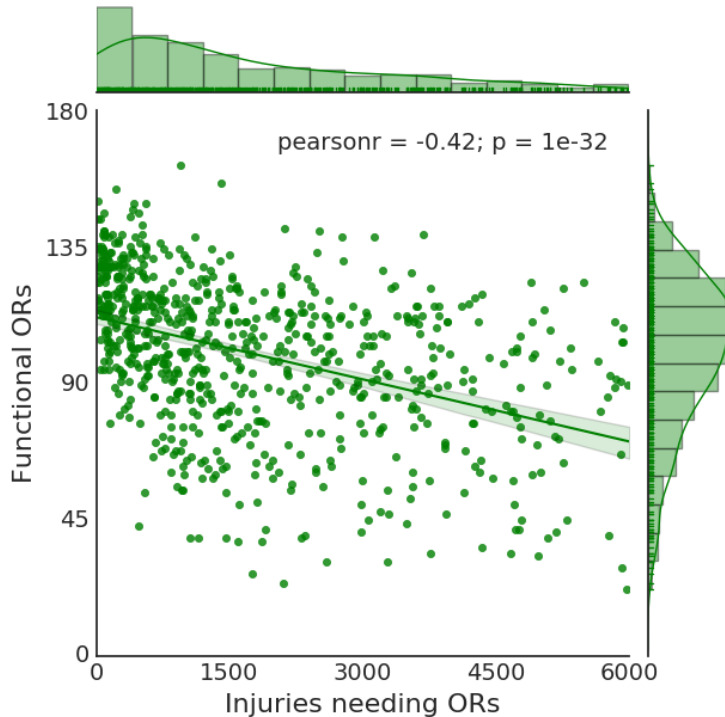


Figure 4: 1,000 simulations of number of casualties needing surgical procedures in operating rooms (ORs) and number of functional operating rooms after the earthquake for the M 8.0 earthquake. The simulations result from probabilistic earthquake modeling (see Methods) and capture uncertainty in ground shaking, building damage, injury occurrence and hospital functionality. The linear trend indicates a negative correlation between the functional ORs and the number of injuries in the simulations.

174 waiting times and effective use of ambulance resources (see Methods). Waiting times are a key
 175 metric to establish necessary patient stabilization procedures until there is an available operating
 176 room in the queue, and the use of ambulances is a complementary measure to ensure that patient
 177 transfers occur effectively. Combining simulations on post-earthquake demand-capacity with data
 178 including the available ambulances at each campus and regular traffic conditions in Lima from
 179 Google Maps API, we conducted a probabilistic evaluation of the system metric performance for
 180 the four emergency plans.

181 1.4 Baseline Strategies with Limited Coordination

182 In the first strategy, hospitals send patients to the closest hospital with functional operating rooms
 183 only if all their operating rooms are non-functional after the earthquake. In this strategy, hospitals
 184 use their own ambulance resources to transfer their patients. This strategy only requires limited
 185 coordination between pairs of hospitals located relatively close to each other, representing an emer-
 186 gency response where the system becomes a set of islands composed of districts or neighborhoods
 187 that treat injuries independently of each other. With this strategy, our mean estimates indicate
 188 that the average waiting time will be 30 days to receive treatment in operating rooms (Figure
 189 6). In some worst-case scenarios, this metric could even increase up to 76 days, as indicated by
 190 the 90th-percentile of this distribution. The 1988 Armenia³⁹ and the 1991 Costa Rica³⁸ earth-

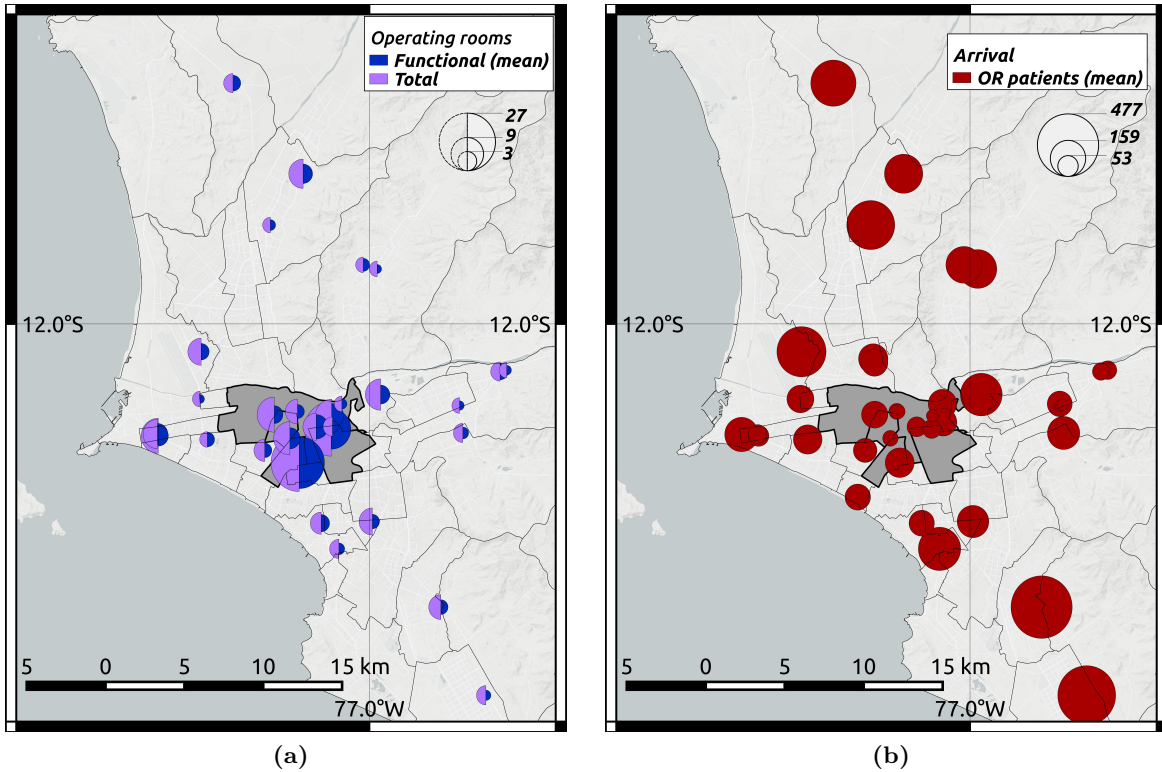


Figure 5: Distribution of operating rooms in Lima. The circle size represents the relative number of operating rooms. (a) Current number of operating rooms in hospital locations¹⁶ and mean estimates of functional operating rooms after the M 8.0 earthquake. (b) Mean estimates of total arrivals of patients who will need surgical procedures after the earthquake.

191 quakes showed that delayed surgical treatment can worsen the patients' health to life-threatening
 192 conditions, for example, those who need resuscitative surgery, e.g., intra-abdominal hemorrhage
 193 or emergency amputation. Thus, such long waiting times in Lima can result in many additional
 194 deaths.

195 For the first strategy, Figure 7a shows the mean estimates of the spatial distribution of treated
 196 patients at each hospital and the patient transfers between hospital pairs. Though this strategy can
 197 offload demands in critical zones, it does not effectively mobilize patients from the lower-capacity
 198 zones to higher-capacity zones. Hospitals with more functional operating rooms treat a similar
 199 number of patients as hospitals with fewer operating rooms. Hospitals in the four centric districts
 200 highlighted previously only treat 1.3k patients, which represents 28% of the demand for operating
 201 rooms, despite having 59% of the total capacity. Additionally, because hospitals do not share
 202 ambulance resources, we find that ambulances are the bottleneck of the system in the periphery.
 203 Hospitals with limited ambulances have to transfer large numbers of patients to offload the high
 204 demand for operating rooms. Thus, if they do not have sufficient ambulance resources, their patients
 205 will lose the opportunity to be treated more promptly in other less crowded hospitals.

206 In the second strategy, hospitals send patients to the hospital with the largest number of func-
 207 tional operating rooms. In this strategy, hospitals send patients only if all their operating rooms are
 208 non-functional and use their own ambulance resources. With this strategy, the mean and the 90th

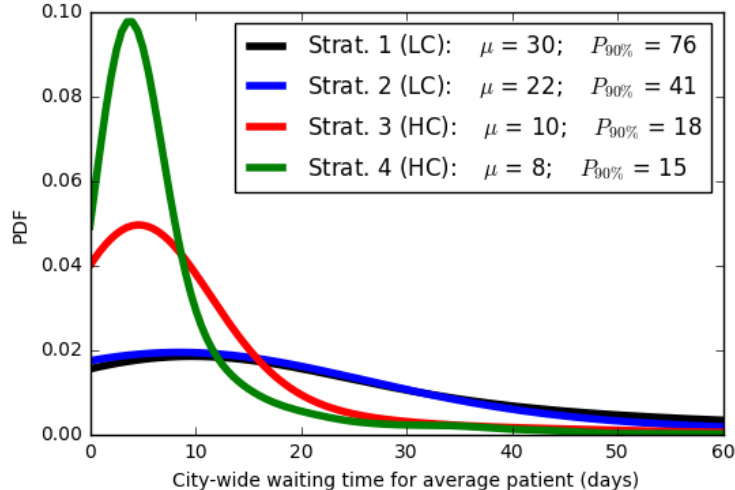


Figure 6: Distribution of city-wide average waiting time for treatment after the earthquake according to four emergency response plans, highlighting mean (μ) and 90th-percentile values ($P_{90\%}$). The time is measured from when the patient is injured by the earthquake until he or she is treated in an operating room. Strategies 1 and 2 are baselines with limited coordination (LC) capacities, whereas strategies 3 and 4 introduce higher coordination (HC) capacities across the whole system level for resource allocation and patient transfers. The ambulance usage and the treatment spatial distribution are show in Figure 7 for each plan.

209 percentile estimates of city-wide waiting time are 22 and 41 days, respectively, outperforming the
 210 first baseline strategy, but not significantly (Figure 6). With this strategy, the system mostly relies
 211 on the largest two hospitals, located in the highlighted centric districts, to meet the demands of
 212 surgical procedures. Figure 7b shows the corresponding distributions of treated patients and trans-
 213 fers. The two largest hospitals treat 2.8k patients, 60% of the total demand, though their functional
 214 operating rooms only constitute 44% of the total. Because multiple hospitals with non-functional
 215 operating rooms send patients to the same large hospitals under this strategy, their operating rooms
 216 overflow. Moreover, such an strategy leads to heavy use of roads from the periphery to the city
 217 center. For example, our mean estimates indicate that 231 patients would have to be transported
 218 from the southernmost hospital alone to the largest hospital, nearly twice as many as the maximum
 219 number of transfers between any hospital pair in the first baseline strategy.

220 1.5 Strategy 3: Sharing Ambulances

221 In the third strategy for effective emergency response, hospitals transfer patients across the system
 222 (see Methods). In addition, they share their ambulance resources across the system. This strategy
 223 represents an emergency plan that requires high coordination at the system level. During the
 224 emergency response following the next big earthquake in Lima, emergency managers could deploy
 225 this policy as soon as they collect information on the actual status of the operating rooms in
 226 hospitals and the actual distributions of injuries, which often takes a few days after the disaster
 227 depending on its magnitude.^{40–43} Using this strategy, the mean and 90-th percentile estimates of
 228 city-wide waiting time are 10 and 19 days, respectively, significantly outperforming the first and
 229 second strategies by factors of 3 and 2.2 in the mean estimates, respectively (Figure 6). Because

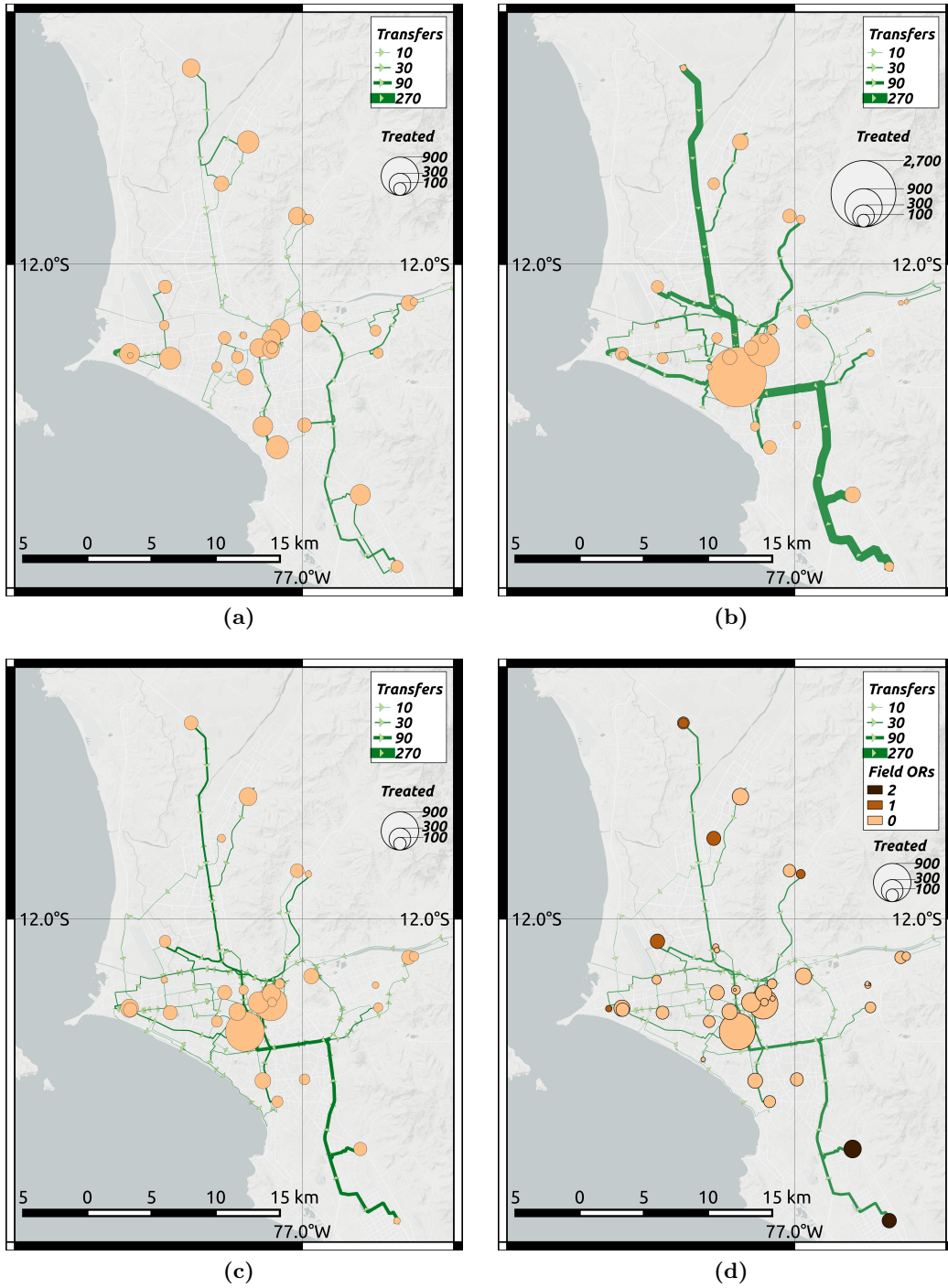


Figure 7: Spatial distribution of patient treatment and transfers. These values represent the average transfers and treated people according to the uncertain distribution of earthquake casualties and residual capacities in the hospital system. (a) Strategy 1: hospitals with unavailable operating rooms can transfer patients to the closest working hospital. (b) Strategy 2: hospitals with unavailable operating rooms can transfer patients to the largest working hospital. (c) Strategy 3: ambulances are shared in the hospital system. (d) Strategy 4: EMTs deploy 15 additional mobile operating rooms during the emergency response. The figure only shows roads between hospital pairs that transferred at least 5 patients.

230 an optimization formulation is used at the system level under this policy, patient transfers are
231 effective at transporting patients from lower-capacity zones to higher-capacity zones, leading to a
232 more effective use of the functional operating rooms across the city.

233 The distribution of treated patients matches the distribution of the residual operating room
234 capacity in the system (Figure 7c). 2.6k people are treated in the hospitals in the four highlighted
235 centric districts, which represents 56% of the total patients in the city and closely approaches the
236 residual capacities in this zone, 59% of the total functional operating rooms. Unlike the second
237 strategy, this strategy does not overload the capacities in the two largest hospitals by sending
238 most patients to them, instead it distributes patients across the system according to the residual
239 capacities of each hospital. Additionally, unlike with the first strategy, ambulance capacities do
240 not bottleneck the system with this policy. Because hospitals share all ambulances in the system,
241 the ambulances will work where they are most needed, from the periphery to the city center. An
242 emergency plan that implements such a strategy will lead to a more balanced use of ambulances
243 through the city and thus it offloads critical roads. With this strategy, close to 90 patients would
244 have to be transported from the southernmost hospital to the largest hospital, less than half the
245 number with the second baseline strategy.

246 1.6 Strategy 4: Deployment of Additional Operating Rooms by EMTs

247 In the fourth policy for effective emergency response, EMTs will deploy 15 additional mobile operat-
248 ing rooms to alleviate high demand-capacity gaps across the system (see Methods). We assume that
249 the additional operating rooms will be functioning three days after the earthquake. This strategy
250 deploys the operating rooms in close proximity to existing hospitals to leverage their triage ar-
251 eas and additional resources such as personnel, power generators or backup water. As with the
252 third strategy, hospitals are also able to share ambulance capacities across the city. Because an
253 optimization formulation is also used, the additional operating rooms are effectively deployed in
254 locations and quantities that are critical to improve the performance of the emergency response.
255 Using this policy, the mean and 90-th percentile estimates of city-wide waiting times are 8 and 15
256 days, respectively (Figure 6). As expected, these estimates outperform the response with the first
257 policy due to the additional operating rooms in the system.

258 Our analysis strategically locates the additional operating rooms in the periphery, mainly in the
259 southernmost and northernmost zones (Figure 7d). By deploying field hospitals in the periphery,
260 more patients can be treated there, offloading the hospitals in the center. With this policy, 2.3k
261 people, representing 48% of the total patients, are treated in the four previously highlighted centric
262 districts, 16% fewer patients than with the first policy. As a result, fewer patients have to be
263 transported from the periphery to the city center, offloading critical roads even more. In this
264 case, the southernmost hospital will only have to transfer 76 patients to the largest hospital, a 17%
265 reduction than with the first policy. If the EMTs deploy more field hospitals using this methodology,
266 then treatment times will be further reduced, the periphery will be better supplied with needed
267 resources, and the usage of ambulances and critical roads will be further offloaded in the city.

268 2 Discussion

269 We present a methodology for characterizing the emergency response of hospital systems after
270 earthquakes and designing policies to treat patients effectively. Our methodology establishes the

271 groundwork for assessing the value of hospital system coordination through a metric that measures
272 the performance of high-coordination emergency policies in terms of waiting times and effective use
273 of hospital resources. Because our methodology considers hospitals in a large urban center behave
274 as a system, emergency managers and resilience officers can apply our methodology to a whole
275 large city and evaluate optimal patient transfer strategies between hospitals, effectively allocate
276 ambulances in the system, and guide the deployment of field hospitals.

277 We found that a M 8.0 earthquake in Lima will cause a spatial distribution of casualties that
278 does not match the post-earthquake capacities of the hospital system (Figure 5). The zones with
279 higher post-earthquake capacity are located in the city center, in clear contrast with the zones
280 with higher post-earthquake demands of health services. Large numbers of patients are located in
281 the periphery, where, unlike the city center, deficient construction practices have rapidly increased
282 the seismic vulnerabilities of the housing infrastructure.⁴⁴ The neighborhoods in the periphery
283 tend to be populated by families with less income and wealth, so the disparities in disaster risk
284 overlap with the economic disparities.⁴⁵ This overlap will exacerbate the critical conditions in
285 the periphery because these families will have less resources to obtain treatment and medicine
286 from private hospitals, relying mostly on public hospitals. During an emergency response, this
287 uneven vulnerability profile in the housing sector exacerbates the resource centralization problem
288 of hospitals in the city, thus leaving the neighborhoods in the periphery predominately underserved
289 during an emergency response. Because in many cities, neighborhoods in peripheral zones have
290 precarious access to health services⁴⁶ and high concentration of seismic vulnerabilities,⁴⁷ these
291 observations in Lima can be extrapolated to multiple urban centers in Latin America and even in
292 developed countries.

293 Emergency planners who aim to treat patients in the city effectively must address these dis-
294 parities by either transporting patients from lower-capacity to higher-capacity zones or supplying
295 the lower-capacity zones with additional resources to meet demands of health services. Though
296 emergency managers can elaborate multiple reasonable strategies to implement such emergency re-
297 sponse measures, our findings shows that strategies based on deeper coordination between hospitals
298 prove to be significantly more effective than the ones with less ability to coordinate (Figure 6).

299 Turning to the two baseline strategies with reduced coordination, both of them have similar low
300 performance even though the system behavior differs fundamentally. Because in the first strategy
301 hospitals transfer patients to the next closest working hospital only when they do not have available
302 operating rooms, ambulance capacities are the bottleneck in some hospitals, whereas they are not
303 even used in other ones. Additionally, the first strategy distributes the number of people treated
304 at each hospital roughly evenly (Figure 7a). Such a treatment distribution results in hospitals
305 with fewer resources treating similar patient numbers as hospitals with more resources, making the
306 system inefficient and increasing waiting times.

307 The second strategy is also a baseline that enables hospitals to transfer patients only to the
308 hospital with the largest number of functional operating rooms in the city. Contrary to the first
309 strategy, the second one distributes the number of treated patients highly unevenly (Figure 7b).
310 Because multiple hospitals often end up transferring patients to the two largest hospitals in the
311 city, these two hospitals largely overflow their capacities. In addition, the second strategy requires
312 heavy use of ambulance resources to transfer patients from the periphery to the city center, where
313 these two largest hospitals are located.

314 In contrast, the third and fourth strategies that have deeper coordination significantly improve
315 the emergency response performance because under these policies, hospitals share resources and

316 leverage strategic system-level information. Because ambulances are shared across the system,
317 they do not bottleneck the system as in first baseline strategy and start to be effectively used in
318 critical zones. Patients are also strategically transferred across the entire hospital system, leading
319 the spatial distribution of treated people matches the post-earthquake capacities of the hospital
320 system (Figure 7c). As a result, the citywide-average waiting times to treat patients decrease
321 quite significantly compared to the previous baseline strategies that only allowed reduced pairwise
322 coordination by factors larger than 2 (Figure 6).

323 In practice, emergency managers will need a few days after the next large earthquake to collect
324 necessary system-level information including both casualties and the residual functionality.^{40–43}
325 However, they can use the trends shown in Figure 7c to establish more informed policies for prag-
326 matic implementation. Emergency planners should use this type of assessment to create earthquake
327 preparedness plans. These plans may include implementing reliable communication lines between
328 hospitals more likely to transfer large number of patients. Additionally, preparedness plans may
329 include a usage prioritization of critical emergency corridors that are more likely to be heavily used
330 by ambulances or an identification of alternative roads in case these corridors have known seismic
331 vulnerabilities.

332 Another advantage of policies with deeper coordination the strategic deployment of EMTs and
333 their additional mobile operating rooms. Besides decreasing waiting times, EMTs that supply oper-
334 ating rooms to the most underserved zones also achieve a more efficient use of ambulances because
335 fewer transfers are needed. EMTs might find it practical to locate these additional operating rooms
336 at the city center, where equipment mobilization is easier and availability of doctors and nurses
337 is higher. However, such a plan may lessen the ability of the hospital system to treat patients
338 because more patients would have to be transferred from the periphery to the center, overloading
339 the roads and potentially overflowing ambulance capacities. Thus, robust earthquake preparedness
340 plans should be developed based on a thorough understanding of the uneven distribution of capac-
341 ity and demand of health services in an earthquake aftermath. Effective plans will capitalize on
342 the methodology and information provided here to better prepare cities facing high significant risk
343 from future large earthquakes.

344 Acknowledgements

345 We thank Abhinav Bindal, Jacqueline Li, and Dr. Maryia Markhvida for helping conceptualize the
346 first version of the patient transfer analysis during an emergency response. We also thank Prof.
347 Sandra Santa Cruz, from the Pontificia Universidad Católica del Perú for granting access to the
348 hospitals’ seismic vulnerability information, and Prof. Carlos Zavala and Miguel Estrada from the
349 Centro Peruano-Japonés de Investigaciones Sísmicas y Mitigación de Desastres (CISMID) and the
350 Universidad Nacional de Ingeniería (UNI) for providing access to the seismic microzonation data in
351 Lima. Additionally, we thank Jill O’Nan for helpful revision of the paper writing. We acknowledge
352 the financial support by the John A. Blume Fellowship from the Civil Engineering Department at
353 Stanford University.

354 3 Methods

355 3.1 Network Flow Model and Optimization Formulation

356 We model the post-earthquake hospital treatment process as a minimum cost time-varying net-
 357 work flow (MCTVNF) problem.^{48,49} In our MCTVNF formulation, a directed graph $G = (N, E)$
 358 represents the hospital system, where $n = |N|$ is the number of graph nodes, and $e = |E|$ is the
 359 number of graph edges. We use a discrete time model with a finite time horizon t_f with time-steps
 360 dt , thus the time $t \in T : \{0, dt, 2dt, \dots, t_f\}$. At each time t , each hospital has two nodes: one
 361 triage node where patients are received into the hospitals, and one discharge node where patients
 362 go after they complete their treatment. Each graph node is associated to an index i and a time
 363 t , where hospitals' triage areas have indexes $i \in \Gamma : \{1, 2, \dots, n_h\}$, and the discharge areas have
 364 indexes $i \in \Lambda : \{n_h + 1, n_h + 2, \dots, 2n_h\}$, where n_h is the number of hospitals in the system. To
 365 define a one-to-one correspondence within the indices of a hospital, if its triage index is $i \in \Gamma$, then
 366 its discharge index is $i + n_h \in \Lambda$. Figure 8 shows an example of a network representation at time
 367 t for a system with three hospitals, where the triage nodes are in red and the discharge nodes in
 368 blue. In this model, the decision variables are both the flows through the edges and the patient
 369 queues in the triage nodes. These variables will track how many patients will stay in triage, be
 370 treated or be transferred to other hospitals.

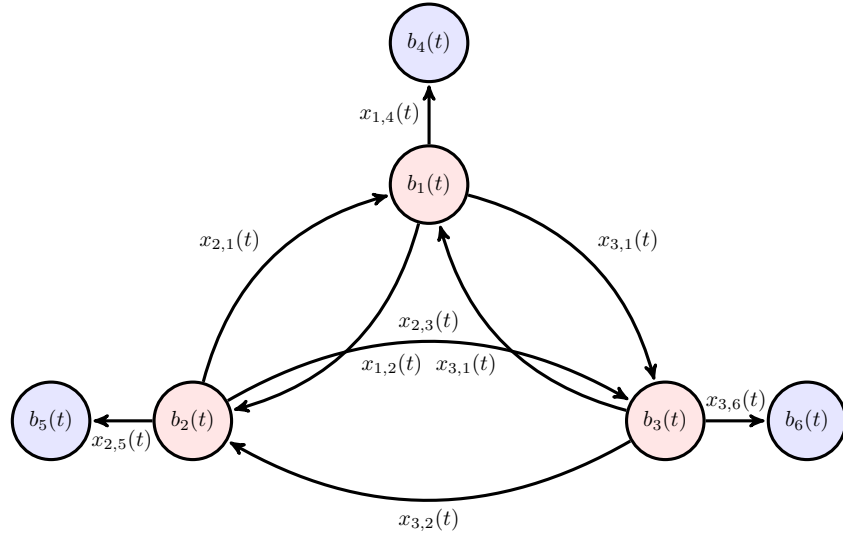


Figure 8: System model with three hospitals at time t as a directed graph. The system model used for the application to Lima has 41 hospitals, i.e., 41 triage and 41 discharge nodes.

371 Each graph node is associated to a time-variant demand-supply variable $b_i(t)$. In triage nodes,
 372 $b_i(t)$ represents the number of people arriving to hospital, thus they are analyzed as source nodes
 373 with nonnegative flows: $b_i(t) \geq 0, \forall i \in \Gamma$. In the discharge nodes, $b_i(t)$ represent the number
 374 of patients who finish their treatment and exit the hospital at time t , thus they are analyzed as
 375 sink nodes with nonpositive flows: $b_i(t) \leq 0, \forall i \in \Lambda$. We assume that patients who finish the
 376 treatment process and exit the hospital do not to return to the hospital system during the time
 377 horizon t_f .

378 Each graph edge is associated to a flow of patients $x_{i,j}(t)$ that leaves node i at time t to go to

node j . In this formulation, edges fully connect the triage nodes to allow hospitals to redistribute their patient loads to potentially any other hospital within the system according to their available ambulances. Additionally, each triage node is connected to its respective discharge node to represent the patient treatment process within a hospital. Figure 8 shows the edges and respective flows between triage nodes from different hospitals and between triage and discharge nodes within same hospitals for the system with three hospitals. At each time t , the flow $x_{i,j}(t)$ has a maximum bound $u_{i,j}(t)$ and a travel time $\tau_{i,j}(t)$. In this discrete formulation, it is considered that the flow $x_{i,j}(t)$ leaves the node i at time t and reaches the node j at time $t + \tau_{i,j}(t)$.

For the edges connecting triage areas, $u_{i,j}(t)$ represents the maximum number of patients who can be transported from triage i to triage j in a different hospital according to the available transportation resources (e.g., ambulances available in the hospital), and $\tau_{i,j}(t)$ is the transportation time of the patients from triage i to triage j . For the application to Lima, $u_{i,j}(t)$ and $\tau_{i,j}(t)$ in these edges were defined according to the ambulance capacities in each hospital and the travel times from pre-earthquake traffic conditions, respectively. When vulnerability data for the transportation system in Lima is available, our model will be able to leverage existing risk models for transportation systems^{50,51} to adjust travel times to post-earthquake traffic conditions.

For the edges connecting triage nodes i with their respective discharge nodes $j = i + n_h$, $u_{i,i+n_h}(t)$ represents the maximum number of patients who can be treated according to the available medical resources for the type and severity of the patients' injuries, and $\tau_{i,i+n_h}(t)$ is the treatment time. For the application to Lima, $u_{i,j}(t)$ and $\tau_{i,j}(t)$ in these edges were defined according to the functional operating rooms in each hospital and average treatment times in operating rooms in previous earthquakes.⁵²

Additionally, we define $y_i(t)$ as a storage variable at each triage node to represent the patients who wait in the hospital queue to either be treated within the hospital or be transported to another hospital with more available resources.

3.1.1 Optimization of Performance Metric

We evaluate both waiting times and effective use of ambulances as the system performance metric, thus the metric includes two objective functions. The first objective function $C_1(X)$ measures waiting time across the city as the average time that a patient would take since the earthquake until completing treatment in the operating room.

$$C_1(X) = \frac{\sum_{t \in T} \sum_{\substack{i \in \Gamma, \\ j = i + n_h}} \{t + \tau_{i,j}\} \times x_{i,j}(t) \times dt}{\sum_{t \in T} \sum_{i \in \Gamma} b_i(t)} \quad (1)$$

X represents a vector containing all the decision variables of flow $x_{i,j}(t)$ in edges and the storage $y_i(t)$ in the triage nodes. The numerator of $C_1(X)$ represents the total number of patients passing through the operating rooms (from each triage node $i \in \Gamma$ to the corresponding discharge node $j = i + n_h \in \Lambda$) multiplied by their respective times to complete treatment, whereas the denominator is the total number of patients arriving to the triage areas. The time horizon t_f is carefully chosen to have enough modeling time to treat the patients. However, in few simulations with significant number of patients and not many functional operating rooms, a couple of terms are added to the numerator, one with the remainder patients in the triage areas, $t_f \times \sum_{i \in \Gamma} y_i(t_f) \times dt$, and another with the remainder patients in the ambulances, $t_f \times \sum_{i \in \Gamma} x_{i,i+n_h}(t_f) \times dt$, in order to properly incorporate the unmet demands at the end of the simulation into $C_1(X)$.

419 The second objective function measures ambulance usage as the total number of patients trans-
 420 ported in ambulances. The objective function $C_2(X)$ is normalized by the total number of patients
 421 analogously to $C_1(X)$.

$$C_2(X) = \frac{\sum_{t \in T} \sum_{i \in \Gamma} \sum_{j \in \Gamma} x_{i,j}(t) \times dt}{\sum_{t \in T} \sum_{i \in \Gamma} b_i(t)} \quad (2)$$

422 We define a system cost $C(X)$ as a weighted sum of $C_1(X)$ and $C_2(X)$ to find a Pareto-optimal
 423 solution.

$$C(X) = \alpha_1 \times C_1(X) + \alpha_2 \times C_2(X) \quad (3)$$

424 After assessing multiple α_1 and α_2 values, we minimized $C(X)$ using values of 0.90 and 0.1,
 425 respectively. Smaller α_2 values resulted in inefficient ambulance usage with small reductions in
 426 waiting times, requiring some patients to be transferred multiple times in ambulances before being
 427 treated. Larger α_2 significantly increased waiting times, thus these α_2 values do not appropriately
 428 represent that the priority in the formulation is to minimize waiting times over to use ambulances
 429 with efficiency. We find the best set of decisions \hat{X} , vector that contains the values of flow variables
 430 $x_{i,j}(t)$ and storage variables $y_i(t)$ which minimize $C(X)$.

$$\hat{X} = \operatorname{argmin}_{x_{i,j}(t); y_i(t)} C(X) \quad (4)$$

431 The decision variables are subject to the constraints in Equations 5, 6, 7, and 8. Equation 5
 432 represents patient flow conservation, which guarantees that all the patients coming into the hospital
 433 system stay within the system until they leave through the discharge nodes.

$$x_{i,i+n_h} + \sum_{j \in \Gamma} x_{i,j}(t) - \sum_{j \in \Gamma} x_{j,i}(t - \tau_{i,j}(t)) + y_i(t + dt) - y_i(t) = b(i), \quad \forall i \in \Gamma, t \in T \quad (5)$$

434 Equations 6 and 7 represent flow capacity constraints. Equation 6 ensures that the people in
 435 the operating rooms do not exceed the unitary capacities $u_{i,i+n_h}$, where $u_{i,i+n_h}$ is estimated as the
 436 number of functional operating rooms in the hospital i over the number of surgeries per day. We
 437 assumed that each surgery takes 4 hours, and that hospitals will be functional 24 hours during the
 438 emergency response using multiple personnel shifts. Such treatment rate equals the rates in foreign
 439 field hospitals after the 2004 Indonesia earthquake/tsunami.⁵²

$$0 \leq \frac{x_{i,i+n_h}(t)}{u_{i,i+n_h}} \leq 1, \quad \forall i \in \Gamma, t \in T \quad (6)$$

440 Equation 7 ensures that the patient transfers do not exceed the total unitary transportation
 441 capacities in a hospital, where $u_{i,j}$ is the unitary capacity if all ambulances of a hospital were only
 442 transferring patients from triage i to j . $u_{i,j}$ equals the number of ambulances in the hospital times
 443 the number of patients transported per ambulance trip over the number of round trips that the an
 444 ambulance can make from triage node i to j . We retrieved travel time information from Google
 445 Maps API to estimate the round trip numbers and assumed that each ambulance trip can take up
 446 to two patients.

$$0 \leq \sum_{j \in \Gamma} \frac{x_{i,j}(t)}{u_{i,j}} \leq 1, \quad \forall i \in \Gamma, t \in T \quad (7)$$

447 Equation 8 ensures that the number of patients waiting in the hospitals' triage queues are
 448 properly represented by a non-negative number.

$$0 \leq y_i(t), \quad \forall i \in \Gamma, t \in T \quad (8)$$

449 Equations 6, 7 and 8 introduce a model relaxation. Whereas the number of patients who
 450 are treated, transported or waiting in the queue can only be non-negative integers, the formulation
 451 expands the variables' domain to include real numbers. This relaxation ensures that the formulation
 452 is tractable. Thus, because the cost and the constraint functions are linear combinations of the
 453 decision variables, we solve this minimization as a linear programming problem using the simplex
 454 algorithm in GLPK of the cvxopt implementation in Python.^{53,54}

455 3.1.2 Model Adaptation for Baseline Strategies 1 and 2

456 Both baseline strategies have limited coordination capacity and only allow each hospital to transfer
 457 patients to only one single hospital with functional operating rooms instead of multiple ones. Thus,
 458 to represent these strategies, the model ignores multiple transfer edges in the flow model, reducing
 459 the elements of the edge set E . In the first baseline strategy, only the edges going from hospitals
 460 without functional operating rooms to the closest hospitals are activated. In the second baseline
 461 strategy, only the edges going from hospitals without functional operating rooms to the hospital
 462 with the are largest number of functional operating rooms are activated.

463 Because the model is solved multiple times according to the number of patients and functional
 464 operating rooms in the earthquake simulation, then the edge connectivity varies from simulation to
 465 simulation. With strategies 1 and 2, the number of edges in the model is significantly reduced, thus
 466 we modeled larger time horizons. We selected a time horizon T_f of 100 days, which is sufficiently
 467 long period to treat all earthquake patients in most simulations, and a time step dt of 1 day.

468 3.1.3 Model Adaptation for Strategy 3: Sharing Ambulances

469 Strategy 3 does not need to disconnect edges in the model. Yet, it modifies the transportation
 470 edges' capacity constraints to enable hospitals to share ambulance resources. Thus, the constraint
 471 in Equation 7 is relaxed as follows.

$$0 \leq \sum_{i \in \Gamma} a_i \sum_{j \in \Gamma} \frac{x_{i,j}(t)}{p_{i,j}} \leq \sum_{i \in \Gamma} a_i, \quad \forall t \in T \quad (9)$$

472 Equation 9 ensures that unitary transportation capacities are not exceeded at a system level at
 473 each time step, where a_i represents the number of ambulances of hospital i . All the other constraints
 474 remain the same. Because modeling this policy requires higher edge connectivity than the baseline
 475 strategies and thus has more computational demands, the time horizon t_f was reduced to 40 days.
 476 It was verified that such a variation did not affect the optimization because less modeling time was
 477 needed as a result of shorter optimal waiting times with the strategies 3 and 4 (Figure 6). The
 478 time step dt was kept equal to 1 day.

479 **3.1.4 Model Adaptation for Strategy 4: Deployment of Additional Operating Rooms**
 480 **by EMTs**

481 Strategy 4 requires an additional modification to the constraint on the operating room capacity in
 482 Equation 6. This strategy allows EMTs to increase hospital capacities by introducing additional
 483 mobile operating rooms in close proximity to them as follows.

$$0 \leq \frac{x_{i,j}(t) - q_i}{u_i} \leq 1, \quad \forall i \in \Gamma, j = i + n_h \in \Lambda, t \in T - \{0, dt, \dots, t_s\} \quad (10)$$

484 Equation 10 ensures that hospitals can increase their unitary operation room capacities by q_i
 485 after the time t_s at which the operating rooms in the field hospitals are deployed in the city. In
 486 addition the sum of the additional resources distributed across the system cannot exceed the total
 487 capacity Q supplied by all the field hospitals in the region as follows.

$$0 \leq \sum_{i \in \Gamma} q_i \leq Q \quad (11)$$

488 All the other constraints remain the same. These modifications barely change the optimization
 489 complexity. Thus, we kept the time horizon equal to 40 days and the time step equal to 1 day.

490 **3.2 Earthquake Casualty Modeling**

491 We utilize an earthquake multiseverity casualty model previously developed by the authors¹⁵ to
 492 evaluate the spatial distribution of injuries requiring surgical treatment after the M 8.0 earthquake.
 493 The model is probabilistic and uses ground shaking estimates to propagate the earthquake inten-
 494 sity to building damage according to the building seismic vulnerability⁵⁵ and the site-specific soil
 495 conditions in Lima.⁵⁶ Next, the model uses information on building occupancy to provide proba-
 496 bilistic estimates of the spatial distribution of injuries and fatalities in the city. The validity of the
 497 model results was verified¹⁴ by comparing the casualties and fatality levels in the city to empirical
 498 formulas¹⁸ and with fatality-to-collapse building data from the 2005 Pakistan earthquake.⁵⁷

499 The model categorizes injuries into three severities. The second- and third-degree severity re-
 500 quire specialized medical attention and hospitalization, however, unlike the second degree, the third
 501 one requires immediate rescue and treatment to avoid death.⁵⁸⁻⁶⁰ We considered that 100% of the
 502 patients with third-degree injuries, for example, having punctured organs or crush syndrome with
 503 exposed wounds, plus 10% of patients with second-degree injuries, for example, having compound
 504 bone fractures, will require surgical treatment in operating rooms. We considered that patients
 505 arrive to the closest hospital during a period of 4 days after the earthquake in accordance to the
 506 evidence from previous earthquakes.^{39,61} Thus, in the flow model the demand-supply variable $b_i(t)$
 507 is larger than 0 in the triage nodes during the first four days after the earthquake. We considered
 508 that patients wait in triage zones to until an operating room is available in the hospital or until
 509 they are transferred to other hospitals.

510 **3.3 Seismic Analysis for hospital functionality**

511 We utilize earthquake simulation to model the functionality of operating rooms during the emer-
 512 gency response.⁶² Hospitals are complex infrastructure, whose post-earthquake functionality de-
 513 pends on multiple components: structural damage; damage in mechanical, electrical components

514 and medical equipment; utility failure; shortage of medical supplies (i.e., oxygen, blood), and short-
515 age of medical personnel.^{7,8,13,63} Hospitals with slight structural damage can lose partial or total
516 functionality as a result of damage and loss of the other components of hospitals.⁶⁴

517 To capture these effects, we analyzed that the structural vulnerability⁵⁵ of the +700 buildings
518 belonging to the 41 healthcare campuses in the city according to the earthquake shaking intensity
519 and the soil conditions on site. Then, we used a Bernoulli distribution to model loss of function-
520 ality that can occur due to failure of components different to the hospitals' structure according
521 the "Hospital Safety Index" (HSI). HSI is based on a qualitative evaluation of multiple hospital
522 components including buildings' nonstructural elements such as equipment and backup medical
523 resources, and technical and organization capacities in the hospitals' personnel.³⁷ HSI has three
524 categories: "A", "B" and "C", ranging from the best to the lowest performance. We used a different
525 Bernoulli distribution for each HSI category. We considered that operating rooms in buildings with
526 no structural damage have 1, 0.75, and 0.5 of functionality probability for categories "A", "B" and
527 "C", respectively, whereas that in buildings with slight structural damage, operating rooms have
528 0.6, 0.45, and 0.3 of functionality probability. Operating rooms in buildings with larger damage
529 levels were considered completely nonfunctional.

530 The 41 campuses in the dataset are part of the public healthcare system led by the Peruvian
531 Health Ministry (MINSA) and the Social Security (Essalud). Even though there is a growing private
532 healthcare system, most of the health care services are provided by the public system in Lima.⁶⁵
533 Physicians who work full time in the public healthcare system often work part-time in the private
534 system,⁶⁶ thus, in an emergency, they would aim to provide services in the public system rather
535 than in the private one. We consider that studying the response of the public sector represents a
536 robust starting point to characterize the earthquake emergency response of the hospital system in
537 Lima.

538 We supplemented the hospitals' building information with the number of ambulance in each
539 hospitals. Because, a few hospitals have no ambulances, we considered that during the emergency
540 response the local government or private institutions will supply one ambulance to each of these
541 hospitals so that each hospital is able to mobilize patients.

542 3.4 Earthquake Shaking

543 We studied the tectonics of the M 8.0 1940 earthquake and located the rupture area in the region
544 delimited by the earthquake aftershock zone.²⁶ We defined the rupture dimensions along the fault
545 strike and dip directions using an empirical function based on subduction zone earthquake data.²⁸

546 Next, we evaluated the ground shaking in a grid of 1kmx1km using site-specific lognormal dis-
547 tributions. We evaluated three ground shaking intensity measures, Peak ground acceleration, *PGA*,
548 spectral acceleration at 0.3s, *Sa(0.3)*, and spectral acceleration at 1s, *Sa(1.0s)*. We selected these
549 intensity measures to better capture the response of multiple typologies of buildings in the inven-
550 tory according to their predominant period of vibration. The log-mean and log-standard-deviation
551 values of the intensity measures were extracted from empirical formulas that relate magnitude, site
552 distance, and soil conditions to the ground shaking.²⁹ We included within-⁶⁷ and between-⁶⁸event
553 correlations in the intensity measures. The between-event correlations introduce spatial correlations
554 to the ground shaking.

555 **3.5 Data Availability**

556 All the data to reproduce the findings of the paper can be found at [https://purl.stanford.edu/
557 dp530wq8437](https://purl.stanford.edu/dp530wq8437).

558 **3.6 Code Availability**

559 All the computer code to reproduce the findings of the paper can also be found at [https://purl.
560 stanford.edu/dp530wq8437](https://purl.stanford.edu/dp530wq8437).

561 **4 Supplementary Information**

562 Lima is a fast-growing megacity with a population close to 10 million people.²¹ Though the center
563 of the city is denser, the peripheral areas of the city have become heavily populated over the last
564 few decades. Currently, close to three million people live in peripheral zones in slums,⁶⁹ where
565 families are low-income, who often start constructing their homes with precarious materials, e.g.,
566 wooden shacks, and then upgrade them to confined-masonry buildings over timespans ranging from
567 a few years to decades.⁷⁰ Figure 9 shows how heavily populated the peripheries are. The popula-
568 tion distribution in this plot represents the average number of people over 24 hours in grids of 1
569 km². Population density is dynamic, but often people spend most time at their residential build-
570 ings, mainly during nighttime. Thus, we considered that this average distribution is a reasonable
571 representation of nighttime population densities.

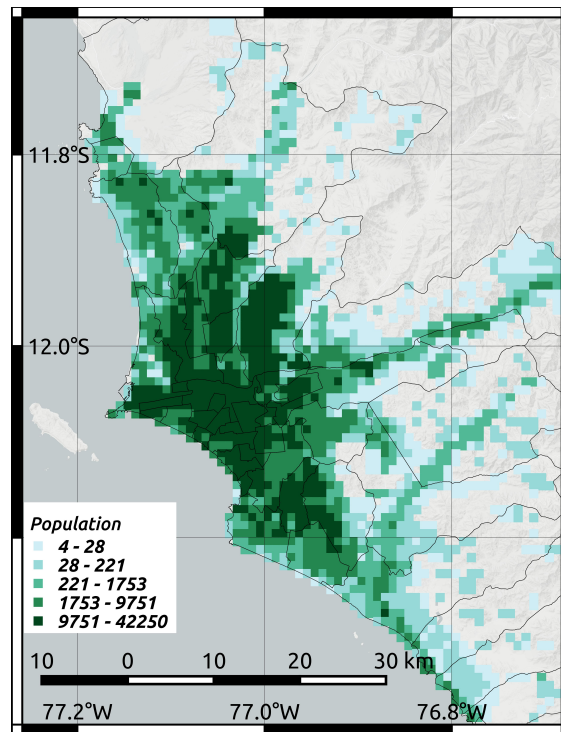


Figure 9: Spatial distribution of population density in Lima per km². Data obtained from LandScan.⁷¹ The intervals in the two plots represent quintiles on the spatial data.

572 The seismic analysis included the assessment of the the number of fatalities and injured people
573 with three types of severities caused by an M 8.0 earthquake occurring at nighttime in Lima, when
574 people are often within their houses. As observed in previous earthquakes, the model considers
575 that most casualties are caused by earthquake damage to buildings in the city. Our mean estimates
576 indicate that the M 8.0 earthquake will cause 60.3k people with injuries of severity 1, 18.9k of
577 severity 2, 2.8k of severity 3, and 5.6k immediate fatalities. People with injuries of severity 1 will
578 require basic medical aid and no hospitalization. People with injuries of severity 2 will require
579 hospital treatment, but the injuries are not life-threatening in the short term, and people with
580 severity 3 will require immediate hospitalization otherwise injuries become life-threatening.^{14,60}

581 Figures 10a and 10b show the mean spatial distributions of injured people with severity 2 and 3 in
582 the city. Because in the model, casualties are result of building damage, the spatial distribution of
583 patients with severity 2 and 3 are heavily cross-correlated and particularly concentrated in areas
584 with large number of buildings that collapse.

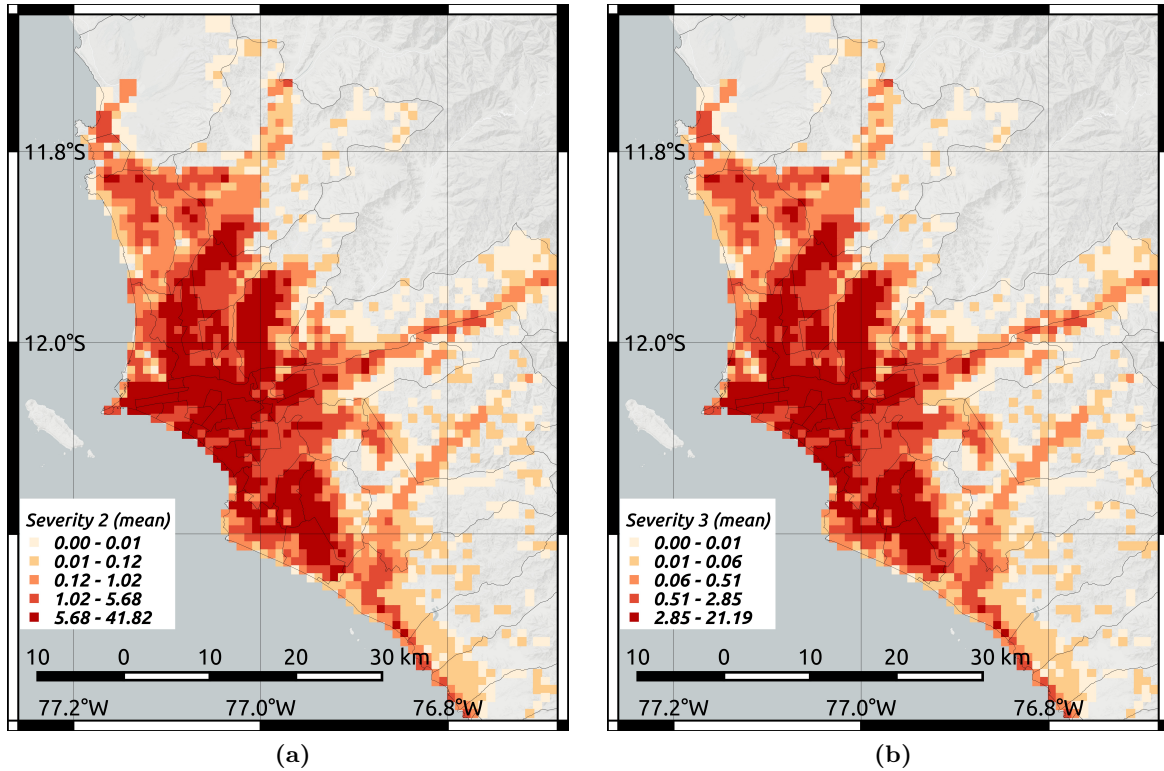


Figure 10: Spatial distribution of patients with a) injuries of severity 2 and b) injuries with severity 3. The intervals in the two plots represent quintiles on the spatial data.

585 The seismic analysis also included the assessment of the ability of hospitals to function after the
586 earthquake. Figure 11 shows the mean functionality ratio of operating rooms in the 41 healthcare
587 campuses that were analyzed. The ratio represents how likely are operating rooms to function
588 after the M 8.0 earthquake considering their structural vulnerabilities, their “HSI” score, and their
589 proneness to experience large shaking intensities as a result of the proximity to the earthquake fault
590 or the soil conditions. Though the absolute number of functional operating rooms was higher at
591 the center of the city, the spatial patterns of of functionality ratios did show a strong prevalence
592 of high ratios in particular zones of the city. Instead of geographical location, construction year
593 was a better indicator of the hospitals’ ability to function, as most newer hospitals showed higher
594 functionality ratios.

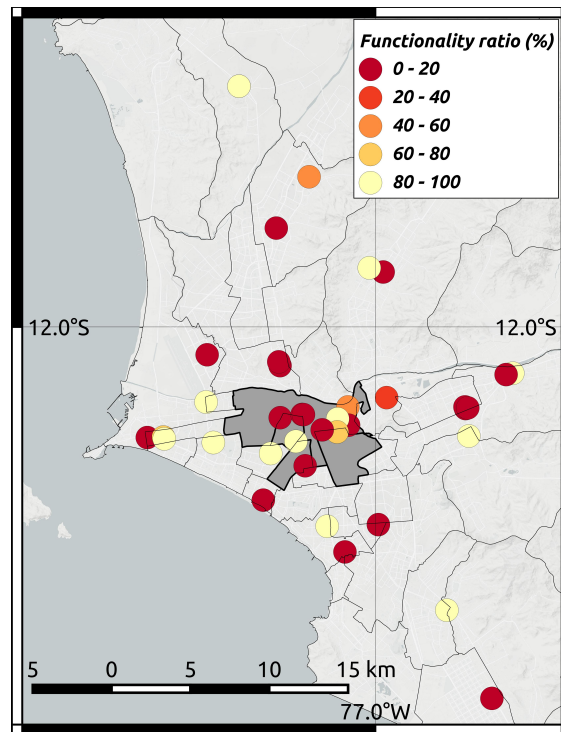


Figure 11: Spatial distribution post-earthquake functionality ratio. Newer hospitals, some of the located in the city center, tend to perform better than the older ones. Few hospitals that did not have operating room capacities under normal conditions were assigned 0% functionality ratio.

References

- 595
596 ¹ National Institute of Standards and Technology (NIST). NIST Special Publication 1190: Com-
597 munity Resilience Planning Guide for Buildings and Infrastructure Systems Volume II. Technical
598 report, National Institute of Standards and Technology (NIST), 2015.
- 599 ² Centre for Research on the Epidemiology of Disasters. EM-DAT — The international disasters
600 database, 2019.
- 601 ³ Robert C. Myrtle, Sami F. Masri, Robert L. Nigbor, and John P. Caffrey. Classification and pri-
602 oritization of essential systems in hospitals under extreme events. *Earthquake Spectra*, 21(3):779–
603 802, 2005.
- 604 ⁴ Pan-American Health Organization (PAHO) - World Health Organization (WHO). Resolution
605 CD50.R15: Plan of Action of Safe Hospitals. In *50th Directory Council, 62nd Session of the*
606 *Regional Committee*, Washington, D.C., USA, 2010.
- 607 ⁵ World Health Organization. A Strategic Framework for Emergency Preparedness. Technical
608 report, Geneva, Switzerland, 2017.
- 609 ⁶ Gian Paolo Cimellaro, Andrei M. Reinhorn, and Michel Bruneau. Performance-based metamodel
610 for healthcare facilities. *Earthquake Engineering & Structural Dynamics*, 41(11):1549–1568, 2011.
- 611 ⁷ Soheil Yavari, M Eeri, Stephanie E Chang, M Eeri, Kenneth J Elwood, and M Eeri. Modeling
612 Post-Earthquake Functionality of Regional Health Care Facilities. 26(3):869–892, 2010.
- 613 ⁸ Caitlin C. Jacques, Jason McIntosh, Sonia Giovinazzi, Thomas D. Kirsch, Thomas Wilson, and
614 Judith Mitrani-Reiser. Resilience of the canterbury hospital system to the 2011 Christchurch
615 earthquake. *Earthquake Spectra*, 30(1):533–554, 2014.
- 616 ⁹ Nicola Tarque, Nicola Liguori, Michelangelo Laterza, Celso Bambaren, Juan Palomino, and San-
617 dra Santa-Cruz. Basic Seismic Response Capability of Hospitals in Lima, Peru. *Disaster Medicine*
618 *and Public Health Preparedness*, pages 1–6, 2018.
- 619 ¹⁰ Jomon Aliyas Paul and Li Lin. Impact of Facility Damages on Hospital Capacities for Decision
620 Support in Disaster Response Planning for an Earthquake. *Prehospital and Disaster Medicine*,
621 24(04):333–341, 2009.
- 622 ¹¹ Pengfei Yi, Santhosh K. George, Jomon Aliyas Paul, and Li Lin. Hospital capacity planning for
623 disaster emergency management. *Socio-Economic Planning Sciences*, 44(3):151–160, 2010.
- 624 ¹² Muhammet Gul and Ali Fuat Guneri. A comprehensive review of emergency department sim-
625 ulation applications for normal and disaster conditions. *Computers and Industrial Engineering*,
626 83:327–344, 2015.
- 627 ¹³ Eric Vugrin, Stephen Verzi, Patrick Finley, Mark Turnquist, Anne Griffin, Karen Ricci, and
628 Tamar Wyte-Lake. Modeling Hospitals’ Adaptive Capacity during a Loss of Infrastructure Ser-
629 vices. *Journal of Healthcare Engineering*, 6(1):85–120, 2015.

- 630 ¹⁴ Luis Ceferino, Anne Kiremidjian, and Gregory Deierlein. Regional Multi-severity Casualty Es-
631 timation Due to Building Damage Following a Mw 8.8 Earthquake Scenario in Lima, Peru.
632 *Earthquake Spectra*, 4(3), 2018.
- 633 ¹⁵ Luis Ceferino, Anne S. Kiremidjian, and Gregory G. Deierlein. Probabilistic Model for Regional
634 Multi-severity Casualty Estimation due to Building Damage Following an Earthquake. *Special*
635 *Collection of ASCE-ASME Journal of Risk and Uncertainty in Engineering Systems: Part A:*
636 *Civil Engineering*, 4(3), 2018.
- 637 ¹⁶ Sandra Santa Cruz, Marcial Blondet, Alejandro Muñoz, Juan Palomino Bendezú, and Rodrigo
638 Tamayo. Evaluación Probabilística de riesgo Sísmico de Escuelas y Hospitales de la ciudad de
639 Lima. Componente 2: Evaluación Probabilística del Riesgo Sísmico de Hospitales en la ciudad
640 de Lima. Technical report, Pontificia Universidad Católica del Perú, Lima, Peru, 2013.
- 641 ¹⁷ Nicola Liguori, Nicola Tarque, Celso Bambarén, Enrico Spacone, Willem Viveen, and Gianpietro
642 de Filippo. Hospital treatment capacity in case of seismic scenario in the Lima Metropolitan
643 area, Peru. *International Journal of Disaster Risk Reduction*, 38(May):101196, 2019.
- 644 ¹⁸ Kishor Jaiswal, David J Wald, and Michael G Hearne. Estimating Casualties for Large Earth-
645 quakes Worldwide Using an Empirical Approach. Technical report, United States Geological
646 Survey (USGS), 2009.
- 647 ¹⁹ Organización Panamericana de la Salud and Organización Mundial de la Salud. NOTA TECNICA
648 Sobre los requisitos mínimos de los Equipos Médicos de Emergencia (EMT) que responden a
649 desastres y emergencias en las Américas. Technical report, 2016.
- 650 ²⁰ World Health Organization (WHO). Minimum Technical Standards and Recommendations
651 for Rehabilitation - Emergency Medical Teams. Technical report, World Health Organization,
652 Geneva, 2016.
- 653 ²¹ Instituto Nacional de Estadísticas e Informática (INEI). Perfil Sociodemográfico de la Provincia
654 de Lima. Technical report, Instituto Nacional de Estadísticas e Informática (INEI), Lima, Peru,
655 2008.
- 656 ²² E. Silgado. Historia de los Sismos más notables en el Perú, 1513-1974. *Instituto Geológico Minero*,
657 page 131, 1978.
- 658 ²³ Lizardo Seiner. *Historia de los sismos en el Perú. Catálogo: Siglos XVIII-XIX*. Universidad de
659 Lima. Fondo Editorial, Lima, Peru, 2011.
- 660 ²⁴ J. C. Villegas-Lanza, M. Chlieh, O Cavalié, H. Tavera, P. Baby, J. Chire-Chira, and J.-M. Noc-
661 quet. Active tectonics of Peru: Heterogeneous interseismic coupling along the Nazca megathrust,
662 rigid motion of the Peruvian Sliver, and Subandean shortening accomodation. *Journal of Geo-*
663 *physical Research : Solid Earth*, pages 1–24, 2016.
- 664 ²⁵ Luis Ceferino, Anne Kiremidjian, and Gregory Deierlein. Probabilistic space- and time-
665 interaction modeling of mainshock earthquake rupture occurrence. *Bulletin of the Seismological*
666 *Society of America*, In review, 2019.

- 667 ²⁶ John a. Kelleher. Rupture zones of large South American earthquakes and some predictions.
668 *Journal of Geophysical Research*, 77(11):2087, 1972.
- 669 ²⁷ L. Dorbath, A. Cisternas, and C. Dorbath. Assessment of the size of large and great historical
670 earthquakes in Peru. *Bulletin of the Seismological Society of America*, 80(3):551–576, 1990.
- 671 ²⁸ F. O. Strasser, M.C. Arango, and J. J. Bommer. Scaling of the Source Dimensions of Interface
672 and Intraslab Subduction-zone Earthquakes with Moment Magnitude. *Seismological Research*
673 *Letters*, 81(6):951–954, 2010.
- 674 ²⁹ Norman Abrahamson, Nicholas Gregor, and Kofi Addo. BC hydro ground motion prediction
675 equations for subduction earthquakes. *Earthquake Spectra*, 32(1):23–44, 2016.
- 676 ³⁰ J. M. Mulvey, S. U. Awan, A. A. Qadri, and M. A. Maqsood. Profile of injuries arising from the
677 2005 Kashmir Earthquake: The first 72 h. *Injury*, 39(5):554–560, 2008.
- 678 ³¹ Tahmasebi Naghi, Kiani Kambiz, Jalali Shahriar, Taheri Afshin, Shahriar Reza, Panjavi Behnam,
679 and Alami Bahador. Musculoskeletal injuries associated with earthquake: A report of injuries of
680 Iran’s December 26, 2003 Bam earthquake casualties managed in tertiary referral centers. *Injury*,
681 36(1):27–32, 2005.
- 682 ³² Sabir Hussain Bhatti, Ishfaq Ahmed, Nazeer Ahmed Qureshi, Maqsood Akram, and Junaid Khan.
683 Head trauma due to earthquake October 2005 - Experience of 300 cases at the combined military
684 hospital Rawalpindi. *Journal of the College of Physicians and Surgeons Pakistan*, 18(1):22–26,
685 2008.
- 686 ³³ M F a Rathore, S Hanif, P W New, A W Butt, M H Aasi, and S-U U Khan. The prevalence
687 of deep vein thrombosis in a cohort of patients with spinal cord injury following the Pakistan
688 earthquake of October 2005. *Spinal Cord*, 46(7):523–526, 2008.
- 689 ³⁴ Wenfang Li, Jun Qian, Xuefen Liu, Qiang Zhang, Lv Wang, Dechang Chen, and Zhaofen Lin.
690 Management of severe crush injury in a front-line tent ICU after the 2008 Wenchuan earthquake
691 in China: an experience with 32 cases. *Critical Care*, 13(6):R178, 2009.
- 692 ³⁵ Carlos Zavala, Claudia Honma, Patricia Gibu, Jorge Gallardo, and Guillermo Huaco. Full Scale
693 on Line Test on Two Story Masonry Building Using Handmade Bricks. *13 th World Conference*
694 *on Earthquake Engineering*, (2885), 2004.
- 695 ³⁶ Luis G. Quiroz, Yoshihisa Maruyama, and Carlos Zavala. Cyclic behavior of Peruvian confined
696 masonry walls and calibration of numerical model using genetic algorithms. *Engineering Struc-*
697 *tures*, 75:561–576, 2014.
- 698 ³⁷ Organización Panamericana de la Salud - Organización Mundial de la Salud. Guía del evaluador
699 Hospitales seguros frente a desastres. Technical report, Washington DC, 2008.
- 700 ³⁸ E A Pretto, D C Angus, J I Abrams, B Shen, R Bissell, V M Ruiz Castro, R Sawyers, Y Wa-
701 toh, N Ceciliano, and E Ricci. An analysis of prehospital mortality in an earthquake. Disaster
702 Reanimatology Study Group. *Prehospital Disaster Med*, 9(2):107–117, 1994.

- 703 ³⁹ Ernesto A. Pretto, Edmund Ricci, Miroslav Klain, Peter Safar, Victor Semenov, Joel Abrams,
704 Samuel Tisherman, David Crippen, and Louise Comfort. Disaster Reanimatology Potentials:
705 A Structured Interview Study in Armenia. III. Results, Conclusions, and Recommendations.
706 *Prehospital and Disaster Medicine*, 7(4):327–337, 1992.
- 707 ⁴⁰ Bruce E. Haynes, Calvin Freeman, Jeffrey L. Rubin, Gus A. Koehler, Shelia M. Enriquez, and
708 Daniel R. Smiley. Medical response to catastrophic events: California’s planning and the Loma
709 Prieta earthquake. *Annals of Emergency Medicine*, 21(4):368–374, 1992.
- 710 ⁴¹ Hiroshi Tanaka, Atsushi Iwai, Oda Jun, Yasuyuki Kuwagata, Tetsuya Matsuoka, Takeshi Shi-
711 mazu, and Toshiharu Yoshioka. Overview of evacuation and transport of patients following the
712 1995 Hanshin-Awaji earthquake. *Journal of Emergency Medicine*, 16(3):439–444, 1998.
- 713 ⁴² Brian Dolan, Anne Esson, Paula Polly Grainger, Sandra Richardson, and Mike Ardagh. Earth-
714 quake disaster response in christchurch, New Zealand. *Journal of emergency nursing: JEN :*
715 *official publication of the Emergency Department Nurses Association*, 37(5):506–9, 2011.
- 716 ⁴³ Lulu Zhang, Xu Liu, Youping Li, Yuan Liu, Zhipeng Liu, Juncong Lin, Ji Shen, Xuefeng Tang,
717 Yi Zhang, and Wannian Liang. Emergency medical rescue efforts after a major earthquake:
718 Lessons from the 2008 Wenchuan earthquake. *The Lancet*, 379(9818):853–861, 2012.
- 719 ⁴⁴ Hildegardo Córdova-Aguilar. la periferia de Lima Metropolitana frente al cambio climático.
720 *Reconociendo las geografías de América Latina y el Caribe*, pages 209–232, 2017.
- 721 ⁴⁵ Instituto Nacional de Estadística e Informática - INEI. Planos Estratificados de Lima Metropoli-
722 tana a Nivel de Manzana 2016 según ingreso per cápita del hogar y según grupos de pobreza
723 monetaria. Technical report, Lima, 2016.
- 724 ⁴⁶ Ricardo Bitrán, Ursula Giedion, Rubi Valenzuela, and Paavo Monkkonen. Keeping Healthy in
725 an Urban Environment: Public Health Challenges for the Urban Poor. In Marianne Fay, editor,
726 *The Urban Poor in Latin America*, number January 2015, chapter 3, pages 179–194. The World
727 Bank, Washington, D.C., 2005.
- 728 ⁴⁷ Global Facility for Disaster Reduction and Recovery (GFDRR) - World Bank. Disaster Risk
729 Management in Latin America and the Caribbean Region: GFDRR Country Notes. Technical
730 report, World Bank, 2012.
- 731 ⁴⁸ Maria Fonoberova. Algorithms for Finding Optimal Flows in Dynamic Networks. In S. Reben-
732 nack, Panos M. Pardalos, Mario V. F. Pereira, and Niko A. Iliadis, editors, *Handbook of Power*
733 *Systems II*, chapter 2. Springer, 2010.
- 734 ⁴⁹ Ebrahim Nasrabadi and S. Mehdi Hashemi. Minimum cost time-varying network flow problems.
735 *Optimization Methods and Software*, 25(3):429–447, 2010.
- 736 ⁵⁰ Mahalia Miller and Jack W Baker. Coupling mode-destination accessibility with seismic risk
737 assessment to identify at-risk communities. *Reliability Engineering and System Safety*, 147:60–
738 71, 2016.
- 739 ⁵¹ Yueyue Fan, Changzheng Liu, Renee Lee, and Anne S. Kiremidjian. Highway Network Retrofit
740 under Seismic Hazard. *Journal of Infrastructure Systems*, 16(3):181–187, 2009.

- 741 ⁵² Johan von Schreeb, Louis Riddez, Hans Samnegård, and Hans Rosling. Foreign Field Hospitals
742 in the Recent Sudden-Onset Disasters in Iran, Haiti, Indonesia, and Pakistan. *Prehospital and*
743 *Disaster Medicine*, 23(02):144–151, 2008.
- 744 ⁵³ M. S. Andersen, J. Dahl, and L. Vandenberghe. CVXOPT: A Python package for convex opti-
745 mization, version 1.2, 2018.
- 746 ⁵⁴ M. S. Andersen, J. Dahl, Z. Liu, and L. Vandenberghe. Interior-point methods for large-scale
747 cone programming. In S. Sra, S. Nowozin, and S. J. Wright, editors, *Optimization for Machine*
748 *Learning*, pages 55–83. MIT Press, 2012.
- 749 ⁵⁵ Mabé Villar-Vega, Vitor Silva, Helen Crowley, Catalina Yepes, Nicola Tarque, Ana Beatriz
750 Acevedo, Matías A. Hube, D. Gustavo Coronel, and Hernán Santa María. Development of
751 a Fragility Model for the Residential Building Stock in South America. *Earthquake Spectra*,
752 33(2):010716EQS005M, 2017.
- 753 ⁵⁶ Diana Calderon. *Dynamic Characteristics of the Soils in Lima, Peru, by estimating Shallow and*
754 *Deep Shear-wave Velocity Profiles*. PhD thesis, Chiba University, 2012.
- 755 ⁵⁷ H Y Noh, Anne Kiremidjian, Luis Ceferino, and Emiliy So. Bayesian Updating of Earthquake
756 Vulnerability Functions with Application to Mortality Rates. *Earthquake Spectra*, 33(3):1173–
757 1189, 2017.
- 758 ⁵⁸ Michael E. Durkin and Charles C. Thiel. Improving Measures to Reduce Earthquake Casualties.
759 *Earthquake Spectra*, 8(1):95–113, 1992.
- 760 ⁵⁹ A W Coburn, R J S Spence, and A Pomonis. Factors determining human casualty levels in
761 earthquakes: Mortality prediction in building collapse. In *Earthquake Engineering, Tenth World*
762 *Conference*, pages 5989–5994, 1992.
- 763 ⁶⁰ Federal Emergency Management Agency (FEMA). Multi-hazard Loss Estimation Methodology:
764 Earthquake Model. Hazus®MH 2.1: Technical Manual., 2015.
- 765 ⁶¹ Shigeaki Baba, Hiroshi Taniguchi, Seiki Nambu, Shuhei Tsuboi, Kenzo Ishihara, and Shuichi
766 Osato. The Great Hanshin Earthquake. *The Lancet*, 347:307–309, 1996.
- 767 ⁶² L Ceferino, A Kiremidjian, and G Deierlein. Computing Hospital System Resilience : a Supply-
768 Demand Perspective. In *11th National Conference on Earthquake Engineering (NCEE)*, Los
769 Angeles, 2018.
- 770 ⁶³ Judith Mitrani-Reiser, Michael Mahoney, William T. Holmes, Juan Carlos De La Llera, Rick
771 Bissell, and Thomas Kirsch. A Functional Loss Assessment of a Hospital System in the Bío-Bío
772 Province. *Earthquake Spectra*, 28(SUPPL.1):473–502, 2012.
- 773 ⁶⁴ Thomas D Kirsch, Judith Mitrani-Reiser, Richard Bissell, Lauren M Sauer, Michael Mahoney,
774 William T Holmes, Nicolás Santa Cruz, and Francisco de la Maza. Impact on hospital func-
775 tions following the 2010 Chilean earthquake. *Disaster medicine and public health preparedness*,
776 4(2):122–128, 2010.

- 777 ⁶⁵ Dirección General de Gestión del Desarrollo de Recursos Humanos. Recursos Humanos en Salud
778 al 2011. Evidencia de Toma de Decisiones. Technical report, Ministerio de Salud del Perú, Lima,
779 2011.
- 780 ⁶⁶ Manuel Jumpa, Stephen Jan, and Anne Mills. The role of regulation in influencing income-
781 generating activities among public sector doctors in Peru. *Human Resources for Health*, 5:1–8,
782 2007.
- 783 ⁶⁷ Katsuichiro Goda and Gail M. Atkinson. Probabilistic characterization of spatially correlated
784 response spectra for earthquakes in Japan. *Bulletin of the Seismological Society of America*,
785 99(5):3003–3020, 2009.
- 786 ⁶⁸ Maryia Markhvida, Luis Ceferino, and Jack W Baker. Modeling spatially correlated spectral
787 accelerations at multiple periods using principal component analysis and geostatistics. *Earthquake*
788 *Engineering and Structural Dynamics*, 2018.
- 789 ⁶⁹ Ben Spencer, Susan Bolton, and Jorge Alarcon. The Informal Urban Communities Initiative:
790 Community-Driven Design in the Slums of Lima, Peru. *International Journal for Service Learning*
791 *in Engineering, Humanitarian Engineering and Social Entrepreneurship*, 9(1):92–107, 2014.
- 792 ⁷⁰ Instituto de Desarrollo Urbano-Cenca. EI Saneamiento Basico en los Barrios Marginales de Lima
793 Metropolitana. Technical report, Programa de Agua y Saneamiento PNUD-Banco Mundial,
794 Lima, 1998.
- 795 ⁷¹ Oak Ridge National Laboratory and Inc. East View Cartographic. East View LandScan global
796 2012, 2013.